nature

https://doi.org/10.1038/s41586-021-04389-z

Accelerated Article Preview

# Considerable escape of SARS-CoV-2 Omicron to antibody neutralization

Received: 10 December 2021

Accepted: 23 December 2021

Accelerated Article Preview Published online 23 December 2021

Cite this article as: Planas, D. et al. Considerable escape of SARS-CoV-2 Omicron to antibody neutralization. *Nature* https://doi.org/10.1038/s41586-021-04389-z (2021).

**Delphine Planas, Nell Saunders, Piet Maes, Florence Guivel-Benhassine, Cyril Planchais, Julian Buchrieser, William-Henry Bolland, Françoise Porrot, Isabelle Staropoli, Frederic Lemoine, Hélène Péré, David Veyer, Julien Puech, Julien Rodary, Guy Baele, Simon Dellicour, Joren Raymenants, Sarah Gorissen, Caspar Geenen, Bert Vanmechelen, Tony Wawina -Bokalanga, Joan Martí-Carreras, Lize Cuypers, Aymeric Sève, Laurent Hocqueloux, Thierry Prazuck, Félix Rey, Etienne Simon-Loriere, Timothée Bruel, Hugo Mouquet, Emmanuel André & Olivier Schwartz**

This is a PDF file of a peer-reviewed paper that has been accepted for publication. Although unedited, the content has been subjected to preliminary formatting. Nature is providing this early version of the typeset paper as a service to our authors and readers. The text and figures will undergo copyediting and a proof review before the paper is published in its final form. Please note that during the production process errors may be discovered which could affect the content, and all legal disclaimers apply.

ACCELERATED ARTICLE PREVIEW

Article

# Considerable escape of SARS-CoV-2 Omicron to antibody neutralization

https://doi.org/10.1038/s41586-021-04389-z

Received: 10 December 2021

Accepted: 23 December 2021

Published online: 23 December 2021

Delphine Planas[1,2,15], Nell Saunders[1,3,15], Piet Maes[4,15], Florence Guivel-Benhassine[1], Cyril Planchais[5], Julian Buchrieser[1], William-Henry Bolland[1,3], Françoise Porrot[1], Isabelle Staropoli[1], Frederic Lemoine[6], Hélène Péré[7,8], David Veyer[7,8], Julien Puech[7], Julien Rodary[7], Guy Baele[4], Simon Dellicour[4,9], Joren Raymenants[10], Sarah Gorissen[10], Caspar Geenen[10], Bert Vanmechelen[4], Tony Wawina -Bokalanga[4], Joan Martí-Carreras[4], Lize Cuypers[11], Aymeric Sève[12], Laurent Hocqueloux[12], Thierry Prazuck[12], Félix Rey[13], Etienne Simon-Loriere[14], Timothée Bruel[1,2,16] ✉, Hugo Mouquet[5,16] ✉, Emmanuel André[10,11,16] ✉ & Olivier Schwartz[1,2,16] ✉

The SARS-CoV-2 Omicron variant was first identified in November 2021 in Botswana and South Africa[1–3]. It has since then spread to many countries and is expected to rapidly become dominant worldwide. The lineage is characterized by the presence of about 32 mutations in the spike, located mostly in the N-terminal domain (NTD) and the receptor binding domain (RBD), which may enhance viral fitness and allow antibody evasion. Here, we isolated an infectious Omicron virus in Belgium, from a traveller returning from Egypt. We examined its sensitivity to 9 monoclonal antibodies (mAbs) clinically approved or in development[4], and to antibodies present in 115 sera from COVID-19 vaccine recipients or convalescent individuals. Omicron was totally or partially resistant to neutralization by all mAbs tested. Sera from Pfizer or AstraZeneca vaccine recipients, sampled 5 months after complete vaccination, barely inhibited Omicron. Sera from COVID-19 convalescent patients collected 6 or 12 months post symptoms displayed low or no neutralizing activity against Omicron. Administration of a booster Pfizer dose as well as vaccination of previously infected individuals generated an anti-Omicron neutralizing response, with titers 6 to 23 fold lower against Omicron than against Delta. Thus, Omicron escapes most therapeutic monoclonal antibodies and to a large extent vaccine-elicited antibodies. Omicron remains however neutralized by antibodies generated by a booster vaccine dose.

In less than three weeks following its discovery, the Omicron variant has been detected in dozens of countries. The WHO has classified this lineage (previously known as Pango lineage B.1.1.529) as a Variant of Concern (VOC) on November 26, 2021[1]. Preliminary estimates of its doubling time range between 1.2 and 3.6 days, in populations with high rate of SARS-CoV-2 immunity[2,5]. Omicron is expected to supplant the currently dominant Delta lineage in the next weeks or months. Little is known about its sensitivity to the humoral immune response. Recent preprints indicated a reduced sensitivity of Omicron to certain monoclonal and polyclonal antibodies[6–10], whereas CD8+ T cell epitopes previously characterized in other variants seem to be conserved in Omicron[11].

## Isolation and characterization of an Omicron variant

We isolated an Omicron variant from a nasopharyngeal swab of an unvaccinated individual that developed moderate symptoms eleven days after returning to Belgium from Egypt. The virus was amplified by one passage on Vero E6 cells. Sequences of the swab and the outgrown virus were identical and identified the Omicron variant (Pango lineage BA.1, GISAID accession ID: (EPI_ISL_6794907 and EPI_ISL_7413964 respectively) (Fig. 1a). The spike protein contained 32 changes, when compared to the D614G strain (belonging to the basal B.1 lineage) used here as a reference, including 7 changes in the N terminal domain (NTD), with substitutions, deletions and a three amino-acid insertion (A67V,

[1]Institut Pasteur, Université de Paris, CNRS UMR3569, Virus and Immunity Unit, 75015, Paris, France. [2]Vaccine Research Institute, 94000, Créteil, France. [3]Université de Paris, École doctorale BioSPC 562, 75013, Paris, France. [4]KU Leuven, Rega Institute, Department of Microbiology, Immunology and Transplantation, Laboratory of Clinical and Epidemiological Virology, Leuven, Belgium. [5]Institut Pasteur, Université de Paris, INSERM U1222, Humoral Immunology Laboratory, 75015, Paris, France. [6]Institut Pasteur, Université de Paris, CNRS USR 3756, Hub de Bioinformatique et Biostatistique, 75015, Paris, France. [7]Hôpital Européen Georges Pompidou, Laboratoire de Virologie, Service de Microbiologie, 75015, Paris, France. [8]Centre de Recherche des Cordelier, INSERM, Université de Paris, Sorbonne Université, Functional Genomics of Solid Tumors (FunGeST), 75006, Paris, France. [9]Université Libre de Bruxelles, Spatial Epidemiology Lab (SpELL), Bruxelles, Belgium. [10]KU Leuven, Department of Microbiology, Immunology and Transplantation, Laboratory Clinical Microbiology, Leuven, Belgium. [11]University Hospitals Leuven, Department of Laboratory Medicine, National Reference Centre for Respiratory Pathogens, Leuven, Belgium. [12]CHR d'Orléans, service de maladies infectieuses, Orléans, France. [13]Institut Pasteur, Université de Paris, CNRS UMR3569, Structural Virology Unit, 75015, Paris, France. [14]Institut Pasteur, Université de Paris, CNRS UMR3569, G5 Evolutionary genomics of RNA viruses, 75015, Paris, France. [15]These authors contributed equally: Delphine Planas, Nell Saunders, Piet Maes. [16]These authors jointly supervised this work: Timothée Bruel, Hugo Mouquet, Emmanuel André, Olivier Schwartz. ✉e-mail: timothee.bruel@pasteur.fr; hugo.mouquet@pasteur.fr; emmanuel.andre@uzleuven.be; olivier.schwartz@pasteur.fr

ACCELERATED ARTICLE PREVIEW

*Δ69-70, T95I, G142D, Δ141-143, Δ211L212I, Ins214EPE*), 15 mutations in the RBD (G339D, S371L, S373P, S375F, K417N, N440K, G446S, S477N, T478K, E484A, Q493R, G496S, Q498R and N501Y, Y505H, the T574K mutation, 3 mutations close to the furin cleavage site (H655Y, N679K and P681H) and 6 in the S2 region (*N764K, D796Y, N856K, Q954H, N969, L981F*) (Fig. 1a). This extensive constellation of changes is unique, but includes at least 11 modifications observed in other lineages and VOCs or at sites mutated in other variants (Fig. 1a). Viral stocks were titrated using S-Fuse reporter cells and Vero cells. S-Fuse cells become GFP+ upon infection, allowing rapid assessment of infectivity and the measurement of neutralizing antibody levels[12–14]. Syncytia were observed in Omicron-infected S-Fuse cells (Extended Data Fig. 1). Syncytia were smaller with Omicron, relative to Delta (Extended Data Fig. 1). Future experiments will help determining whether the fusogenic potential of Omicron is different from that of other variants[15].

### Phylogenetic analysis of the Omicron lineage

We inferred a global phylogeny subsampling SARS-CoV-2 sequences available on the GISAID EpiCoV database. To better contextualize the isolated virus genome, we performed a focused phylogenetic analysis using as background all Omicron samples deposited on GISAID on December 6, 2021, (Extended Data Fig. 2). The tree topology indicates that the Omicron lineage does not directly derive from any of the previously described VOCs. The very long branch of the Omicron lineage in the time-calibrated tree (Extended Data Fig. 2) might reflect a cryptic and potentially complex evolutionary history. At the time of writing, no Omicron genomic sequences from Egypt were available on GISAID, nor do we know of any sequences of travellers that used the same planes. The isolated strain genome showed no close connection to other Belgian Omicron infections. Follow-up analyses with additional genomic data will improve phylogenetic resolution to determine whether the patient was infected before or after returning to Belgium.

### Mutational landscape in Omicron

We highlighted the 29 amino acid substitutions, the 3 amino-acid deletions and a 3-residue insertion present in the Omicron spike, with respect to the Wuhan strain, in a 3D model of the protein (Extended Data Fig. 3a). The 15 mutations in the RBD cluster around the trimer interface. The RBD is the target of the most potently neutralizing monoclonal antibodies (mAbs) against SARS-CoV-2, which have been divided into four classes depending of the location of their epitope[4,16,17] (Extended Data Fig. 3b). mAbs in classes 1 and 2 compete for hACE2 binding, whereas those from classes 3 and 4 bind away from the hACE2 interaction surface (Extended Data Fig. 3b). The epitopes of the class 2 and 3 mAbs are exposed irrespective of the conformation of the RBD on the spike (Up or Down configuration[18] while those of classes 1 and 4 require an RBD in the Up conformation. Whereas the previous variants of concern (VOCs) displayed mutations only in the region targeted by class 1 and 2 mAbs, Omicron mutations are located within the epitopes of all four classes of mAbs. The mutations, insertion and deletions in the NTD might also impact recognition of this domain by antibodies.

### Neutralization of Omicron by monoclonal antibodies

We then assessed the sensitivity of Omicron to a panel of human mAbs using the S-Fuse assay. We tested 9 antibodies in clinical use or in development[19–25]. These mAbs belong to the 4 main classes of anti-RBD antibodies[4,16,17]. Bamlanivimab and Etesevimab (class 2 and class 1, respectively) are mixed in the Lilly cocktail. Casirivimab and Imdevimab (class 1 and class 3, respectively) form the REGN-COV2 cocktail from Regeneron and Roche (Ronapreve™). Cilgavimab and Tixagevimab (class 2 and class 1, respectively) from AstraZeneca are also used in combination (Evusheld™). Regdanvimab (Regkirona™) (Celltrion) is a class 1 antibody. Sotrovimab (Xevudy™) by GlaxoSmithKline and Vir Biotechnology is a class 3 antibody that displays activity against diverse coronaviruses. It targets an RBD epitope outside the receptor binding motif, which includes N343-linked glycans. Adintrevimab (ADG20) developed by Adagio binds to an epitope located in between the class 1 and class 4 sites.

We measured the activity of the 9 antibodies described above against Omicron and included the Delta variant for comparison purposes (Fig. 1b). As previously reported, Bamlanivimab did not neutralize Delta[14,26,27]. The other antibodies neutralized Delta with IC50 (Inhibitory Concentration 50%) varying from 3.1 to 325 ng/mL (Fig. 1b and Extended Data Fig. 4). Five antibodies (Bamlanivimab, Etesevimab, Casirivimab, Imdevimab and Regdanvimab) lost antiviral activity against Omicron. The four other antibodies displayed a 2.8 to 453-fold increase of IC50 (ranging from 403 to 8305 ng/ml) against Omicron. Sotrovimab was the only antibody displaying a rather similar activity against both strains, with a IC50 of 325 and 917 ng/mL against Delta and Omicron, respectively. We also tested the antibodies in combination, to mimic the therapeutic cocktails. Bamlanivimab+Etesevimab (Lilly) or Casirivimab+Imdevimab (Ronapreve™) were inactive against Omicron. Cilgavimab+Tixagevimab (Evusheld™) neutralized Omicron with an IC50 of 773 ng/mL, corresponding to a 58-fold increase relative to Delta (Fig. 1b and Extended Data Fig. 4).

We next examined by flow cytometry the binding of each mAb to Vero cells infected with Delta and Omicron variants (Extended Data Fig. 4). The five clinical antibodies that lost antiviral activity (Bamlanivimab, Etesevimab, Casirivimab, Imdevimab and Regdanvimab) displayed a strong reduction (8-47 fold and 11-242 fold, at 1 and 0.1 μg/mL,respectively) in their binding to Omicron infected cells, when compared to Delta-infected cells, as measured by the Median Fluorescence Intensity (MFI) of the signal (Extended Data Fig. 4). Cilgavimab, Sotrovimab, Tixagevimab and Andinrevimab that remained partly active were less impaired in their binding to Omicron-infected cell (2 to 9 fold and 1.6 to 11 fold decrease, at 1 and 0.1 μg/mL, respectively) (Extended Data Fig. 4).

Thus, Omicron totally or partially escapes neutralization by the tested antibodies. Our results are in line with recent preprints[7,8,10]. The neutralization escape correlates with a reduction of binding of the antibodies to the Omicron spike.

### Sensitivity of Omicron to sera from vaccinees

We next asked whether vaccine-elicited antibodies neutralized Omicron. To this aim, we randomly selected 54 individuals from a cohort established in the French city of Orléans, composed of vaccinated subjects that were not previously infected with SARS-CoV-2. The characteristics of vaccinees are depicted in Extended Data Table 1. Sixteen individuals received the Pfizer two-dose vaccine regimen and 18 the Astrazeneca two-dose vaccine regimen. 20 individuals vaccinated with Pfizer received a booster dose. We measured the potency of their sera against the Delta and Omicron strains. We used as a control the D614G ancestral strain (belonging to the basal B.1 lineage) (Fig. 2a). We calculated the ED50 (Effective Dose 50%) for each combination of serum and virus. Sera were first sampled 5 months after the full two-dose vaccination. With the Pfizer vaccine, the levels of neutralizing antibodies were relatively low against D614G and Delta (median ED50 of neutralization of 329 and 91), reflecting the waning of the humoral response[14] (Fig. 2a). We did not detect any neutralization against the Omicron variant with these sera, except one which displayed a low antiviral activity (Fig. 2a). The percentage of sera with a detectable neutralizing activity is presented in Extended Data Fig. 5.

A similar pattern was observed with the AstraZeneca vaccine. Five months after vaccination, the levels of antibodies neutralizing Delta were low (ED50 of 187 and 68 against D614G and Delta, respectively). No antiviral activity was detected against Omicron in 90% of the sera (Fig. 2a and Extended Data Fig. 5).

We next examined the impact of a Pfizer booster dose, administrated 7 months after Pfizer vaccination. The sera were collected one month (M1) after the third dose. The booster dose enhanced neutralization titers against D614G and Delta by 39 and 49 fold (ED50 12739 and 4489,

ACCELERATED ARTICLE PREVIEW

respectively, when compared to the M5 sampling time). It was also associated with strong increase of the neutralization activity against Omicron (ED50 of 722) (Fig. 2b). 100% of the tested sera displayed a neutralizing activity at this time point (Extended Data Fig. 5).

Altogether, these results indicate that Omicron is poorly or not neutralized by vaccinees' sera sampled 5 months after vaccination. The booster dose triggered a detectable cross-neutralization activity against Omicron. However, even after the booster dose the variant displayed a reduction of ED50 of 18 and 6 fold, when compared to D614G and Delta, respectively.

### Sensitivity of Omicron to sera from convalescents

We subsequentely examined the neutralization ability of sera from convalescent subjects. We randomly selected 61 longitudinal samples from 40 donors in a cohort of infected individuals from Orléans. Individuals were diagnosed with SARS-CoV-2 infection by RT-qPCR (Extended table 2b). We previously studied the potency of these sera against D614G, Alpha, Beta and Delta isolates[13,14]. We analyzed individuals sampled at a median of 6 and 12 months (M6 and M12) post onset of symptoms (POS). With the D614G and Delta variants, the neutralization titers were stable or slightly decreased overtime (569 and 580 for D614G, 235 and 143 for Delta, at M6 and M12, respectively)[13] (Fig. 2c). The convalescent sera barely neutralized or did not inhibit at all Omicron at these time points. Only 36% and 39% of the samples displayed a neutralizing activity against Omicron at M6 and M12, respectively, whereas the majority (91-94%) were active against Delta (Extended Data Fig. 5).

Twenty two individuals were vaccinated at M12 with a Pfizer dose. Sera sampled one month after vaccination showed a drastic increase in neutralizing antibody titers against the D614G and Delta variants, reaching a median ED50 of 78162 and 33536, respectively (Fig. 2d). These sera also neutralized Omicron, with a median ED50 of 1466 (Fig. 2d). Therefore, as shown with other variants[13,28,29], a single dose of vaccine boosted cross-neutralizing antibody responses to Omicron in previously infected individuals. The neutralization titers were however reduced by 53 and 23 fold, when compared to D614G and Delta, respectively.

## Discussion

Omicron has opened a new chapter in the COVID-19 pandemic[2,30]. The principal concerns about this variant include its high transmissibility, as underlined by its rapid spread in different countries, and the presence of over 55 mutations spanning the whole viral genome. Omicron contains 32 mutations in the spike, lying in the NTD, RBD and in vicinity of the furin cleavage site. Some mutations were already present in other VOCs and VOIs, and have been extensively characterized[30–32]. Due to their position, they are expected to affect the binding of natural or therapeutic antibodies, to increase affinity to ACE2 and to enhance the fusogenic activity of the spike. Future work will help determining how this association of mutations impacts viral fitness in culture systems and their contribution to the high transmissibility of the variant.

Here, we studied the cross-reactivity of clinical or pre-clinical mAbs, as well as of 115 sera from vaccine recipients and long-term convalescent individuals against an infectious Omicron isolate. We report that among nine mAb in clinical use or in development, six (Bamlanivimab, Etesevimab, Casirivimab, Imdevimab, Tixagevimab and Regdanvimab) were inactive against Omicron. Two other antibodies (Cilgavimab, Andintrevimab) displayed about a 20-fold increase of IC50. Sotrovimab was less affected by Omicron's mutations, with an IC50 increased by only 3 fold. We also show that Omicron was barely neutralized by sera from vaccinated individuals sampled 5 months after administration of two doses of Pfizer or AstraZeneca vaccine. Sera from convalescent individuals at 6 or 12 months post infection barely neutralized or did not detectably neutralize Omicron.

The decrease of antibody efficacy helps explaining the high number of breakthrough infections and reinfection cases, and the spread of Omicron in both non-immune and immune individuals[33]. There is currently no evidence of increased disease severity associated with Omicron compared with Delta, either among naïve or immunized individuals. It is likely that even if pre-existing SARS-CoV-2 antibodies may poorly prevent Omicron infection, anamnestic responses and cellular immunity will be operative to prevent severe forms of the disease[34].

We further report that a booster dose of Pfizer vaccine, as well as vaccination of previously infected individuals, strongly increased overall levels of anti-SARS-CoV-2 neutralizing antibodies, well above a threshold allowing inhibition of Omicron. Affinity maturation of antibodies is known to improve the efficacy of the humoral anti-SARS-CoV-2 response overtime[35,36]. This process helps explaining the efficacy of booster doses in immune patients. However, sera with high antibody levels displayed a 6 to 23 fold reduction in neutralization efficacy against Omicron, when compared to the currently predominant Delta strain.

Potential limitations of our work include a low number of vaccine recipients and convalescents sera analyzed and the lack of characterization of cellular immunity, which is known to be more cross-reactive than the humoral response. Our results may therefore partly underestimate the residual protection offered by vaccines and previous infections against Omicron infection, in particular with regard to the severity of disease. We only analyzed sera sampled 1 month after the booster dose, or after vaccination of infected individuals. Future work with more individuals and longer survey periods will help characterize the duration of the humoral response against Omicron. We focused on immune responses elicited by Pfizer and AstraZeneca vaccination. It will be worth determining the potency of other vaccines against this variant.

We focused our analyses on one single viral isolate, corresponding to the archetype Omicron variant sequence (Pango BA.1 lineage). Two related lineages with additional mutations (BA.2 and BA.3) have recently emerged and are less widely spread. It will be worth comparing the behavior of viral isolates from these more recent lineages to the main BA.1 Omicron strain.

Our results have important public health consequences regarding the use of therapeutic mAbs and vaccines. Clinical indications of mAbs include pre-exposure prophylaxis in individuals unable to mount an immune response, as well as prevention of COVID-19 in infected individuals at high risk for evolution towards severe disease. Antibody-based treatment strategies need to be rapidy adapted to Omicron. Experiments in preclinical models or clinical trials are warranted to assess whether the drops in IC50 are translated into impaired clinical efficacy of the mAbs that retain efficacy against Omicron. Most of the low-income countries display a weak vaccination rate, a situation that likely facilitates SARS-CoV-2 spread and continuous evolution. A booster dose significantly improves the quality and the level of the humoral immune response, and is associated with a strong protection against severe forms of the disease[37]. An accelerated deployment of vaccines and boosters throughout the world is necessary to counteract viral spread. Our results also suggest that there is a need to update and complete the current pharmacopoeia, in particular with regard to vaccines and mAbs.

## Online content

Any methods, additional references, Nature Research reporting summaries, source data, extended data, supplementary information, acknowledgements, peer review information; details of author contributions and competing interests; and statements of data and code availability are available at https://doi.org/10.1038/s41586-021-04389-z.


1. WHO. https://www.who.int/news/item/26-11-2021-classification-of-omicron-(b.1.1.529)-sars-cov-2-variant-of-concern. (2021).
2. Karim, S. S. A. & Karim, Q. A. Omicron SARS-CoV-2 variant: a new chapter in the COVID-19 pandemic. *The Lancet* **398**, 2126-2128, https://doi.org/10.1016/S0140-6736(21)02758-6 (2021).


ACCELERATED ARTICLE PREVIEW

3. Viana, R. et al. Rapid epidemic expansion of the SARS-CoV-2 Omicron variant in southern Africa. *medRxiv*, 2021.2012.2019.21268028, https://doi.org/10.1101/2021.12.19.21268028 (2021).
4. Taylor, P. C. et al. Neutralizing monoclonal antibodies for treatment of COVID-19. *Nature Reviews Immunology* **21**, 382-393, https://doi.org/10.1038/s41577-021-00542-x (2021).
5. Grabowski, F., Kochańczyk, M. & Lipniacki, T. Omicron strain spreads with the doubling time of 3.2—3.6 days in South Africa province of Gauteng that achieved herd immunity to Delta variant. *medRxiv*, 2021.2012.2008.21267494, https://doi.org/10.1101/2021.12.08.21267494 (2021).
6. Cele, S. et al. SARS-CoV-2 Omicron has extensive but incomplete escape of Pfizer BNT162b2 elicited neutralization and requires ACE2 for infection. *medRxiv*, 2021.2012.2008.21267417, https://doi.org/10.1101/2021.12.08.21267417 (2021).
7. Xiaoliang, X. et al. *Nature Portfolio*, https://doi.org/10.21203/rs.3.rs-1148985/v1 (2021).
8. Cameroni, E. et al. Broadly neutralizing antibodies overcome SARS-CoV-2 Omicron antigenic shift. *Biorxiv*, 2021.2012.2012.472269, https://doi.org/10.1101/2021.12.12.472269 (2021).
9. Dejnirattisai, W. et al. Reduced neutralisation of SARS-COV-2 Omicron-B.1.1.529 variant by post-immunisation serum. *medRxiv*, 2021.2012.2010.21267534, https://doi.org/10.1101/2021.12.10.21267534 (2021).
10. Aggarwal, A. et al. SARS-CoV-2 Omicron: evasion of potent humoral responses and resistance to clinical immunotherapeutics relative to viral variants of concern. *medRxiv*, 2021.2012.2014.21267772, https://doi.org/10.1101/2021.12.14.21267772 (2021).
11. Redd, A. D. et al. Minimal cross-over between mutations associated with Omicron variant of SARS-CoV-2 and CD8+ T cell epitopes identified in COVID-19 convalescent individuals. Preprint at *Biorxiv* https://doi.org/10.1101/2021.12.06.471446 (2021).
12. Buchrieser, J. et al. Syncytia formation by SARS-CoV-2 infected cells. *The EMBO Journal*, **39**, e106267, https://doi.org/10.15252/embj.2020106267 (2020).
13. Planas, D. et al. Sensitivity of infectious SARS-CoV-2 B.1.1.7 and B.1.351 variants to neutralizing antibodies. *Nature Medicine*, **27**, 917-924, https://doi.org/10.1038/s41591-021-01318-5 (2021).
14. Planas, D. et al. Reduced sensitivity of SARS-CoV-2 variant Delta to antibody neutralization. *Nature*, https://doi.org/10.1038/s41586-021-03777-9 (2021).
15. Rajah, M. M. et al. SARS-CoV-2 Alpha, Beta, and Delta variants display enhanced Spike-mediated syncytia formation. *The EMBO Journal* **n/a**, e108944, https://doi.org/10.15252/embj.2021108944 (2021).
16. Liu, L. et al. Potent neutralizing antibodies against multiple epitopes on SARS-CoV-2 spike. *Nature* **584**, 450-456, https://doi.org/10.1038/s41586-020-2571-7 (2020).
17. Barnes, C. O. et al. SARS-CoV-2 neutralizing antibody structures inform therapeutic strategies. *Nature* **588**, 682-687, 10.1038/s41586-020-2852-1 PMID - 33045718 (2020).
18. Wrapp, D. et al. Cryo-EM structure of the 2019-nCoV spike in the prefusion conformation. *Science* **367**, 1260-1263, https://doi.org/10.1126/science.abb2507 (2020).
19. Rappazzo, C. G. et al. Broad and potent activity against SARS-like viruses by an engineered human monoclonal antibody. *Science* **371**, 823-829, https://doi.org/10.1126/science.abf4830 (2021).
20. Zost, S. J. et al. Potently neutralizing and protective human antibodies against SARS-CoV-2. *Nature* **584**, 443-449, https://doi.org/10.1038/s41586-020-2548-6 (2020).
21. Kim, C. et al. A therapeutic neutralizing antibody targeting receptor binding domain of SARS-CoV-2 spike protein. *Nature Communications* **12**, 288, https://doi.org/10.1038/s41467-020-20602-5 (2021).
22. Shi, R. et al. A human neutralizing antibody targets the receptor-binding site of SARS-CoV-2. *Nature* **584**, 120-124, https://doi.org/10.1038/s41586-020-2381-y (2020).
23. Jones, B. E. et al. The neutralizing antibody, LY-CoV555, protects against SARS-CoV-2 infection in nonhuman primates. *Science Translational Medicine* **13**, eabf1906, https://doi.org/10.1126/scitranslmed.abf1906 (2021).
24. Hansen, J. et al. Studies in humanized mice and convalescent humans yield a SARS-CoV-2 antibody cocktail. *Science* **369**, 1010-1014, https://doi.org/10.1126/science.abd0827 (2020).
25. Pinto, D. et al. Cross-neutralization of SARS-CoV-2 by a human monoclonal SARS-CoV antibody. *Nature* **583**, 290-295, https://doi.org/10.1038/s41586-020-2349-y (2020).
26. Liu, J. et al. BNT162b2-elicited neutralization of B.1.617 and other SARS-CoV-2 variants. *Nature*, https://doi.org/10.1038/s41586-021-03693-y (2021).
27. Lucas, C. et al. Impact of circulating SARS-CoV-2 variants on mRNA vaccine-induced immunity. *Nature*, **600**, 523-529 (2021).
28. Gallais, F. et al. Anti-SARS-CoV-2 Antibodies Persist for up to 13 Months and Reduce Risk of Reinfection. *medRxiv*, 2021.2005.2007.21256823, https://doi.org/10.1101/2021.05.07.21256823 (2021).
29. Krammer, F. et al. Antibody Responses in Seropositive Persons after a Single Dose of SARS-CoV-2 mRNA Vaccine. *New England Journal of Medicine* **384**, 1372-1374, https://doi.org/10.1056/NEJMc2101667 (2021).
30. McCallum, M. et al. SARS-CoV-2 immune evasion by the B.1.427/B.1.429 variant of concern. *Science*, **373**, 648-654, https://doi.org/10.1126/science.abi7994 (2021).
31. Plante, J. A. et al. The variant gambit: COVID-19's next move. *Cell Host & Microbe* **29**, 508-515, https://doi.org/10.1016/j.chom.2021.02.020 (2021).
32. Starr, T. N. et al. Prospective mapping of viral mutations that escape antibodies used to treat COVID-19. *Science* **371**, 850-854, https://doi.org/10.1126/science.abf9302 (2021).
33. Pulliam, J. R. C. et al. Increased risk of SARS-CoV-2 reinfection associated with emergence of the Omicron variant in South Africa. *medRxiv*, 2021.2011.2011.21266068, https://doi.org/10.1101/2021.11.11.21266068 (2021).
34. Gagne, M. et al. Protection from SARS-CoV-2 Delta one year after mRNA-1273 vaccination in rhesus macaques is coincident with anamnestic antibody response in the lung. *Cell*, https://doi.org/10.1016/j.cell.2021.12.002 (2021).
35. Gaebler, C. et al. Evolution of antibody immunity to SARS-CoV-2. *Nature*, **591**, 639-644, https://doi.org/10.1038/s41586-41021-03207 (2021).
36. Wang, Z. et al. Naturally enhanced neutralizing breadth against SARS-CoV-2 one year after infection. *Nature* **595**, 426-431, https://doi.org/10.1038/s41586-021-03696-9 (2021).
37. Barda, N. et al. Effectiveness of a third dose of the BNT162b2 mRNA COVID-19 vaccine for preventing severe outcomes in Israel: an observational study. *The Lancet*, **398**, 2093-2100, https://doi.org/10.1016/S0140-6736(21)02249-2 (2021).
38. Tzou, P. L. et al. Coronavirus Antiviral Research Database (CoV-RDB): An Online Database Designed to Facilitate Comparisons between Candidate Anti-Coronavirus Compounds. *Viruses* **12**, 1006 (2020).

**Publisher's note** Springer Nature remains neutral with regard to jurisdictional claims in published maps and institutional affiliations.

© The Author(s), under exclusive licence to Springer Nature Limited 2021

ACCELERATED ARTICLE PREVIEW

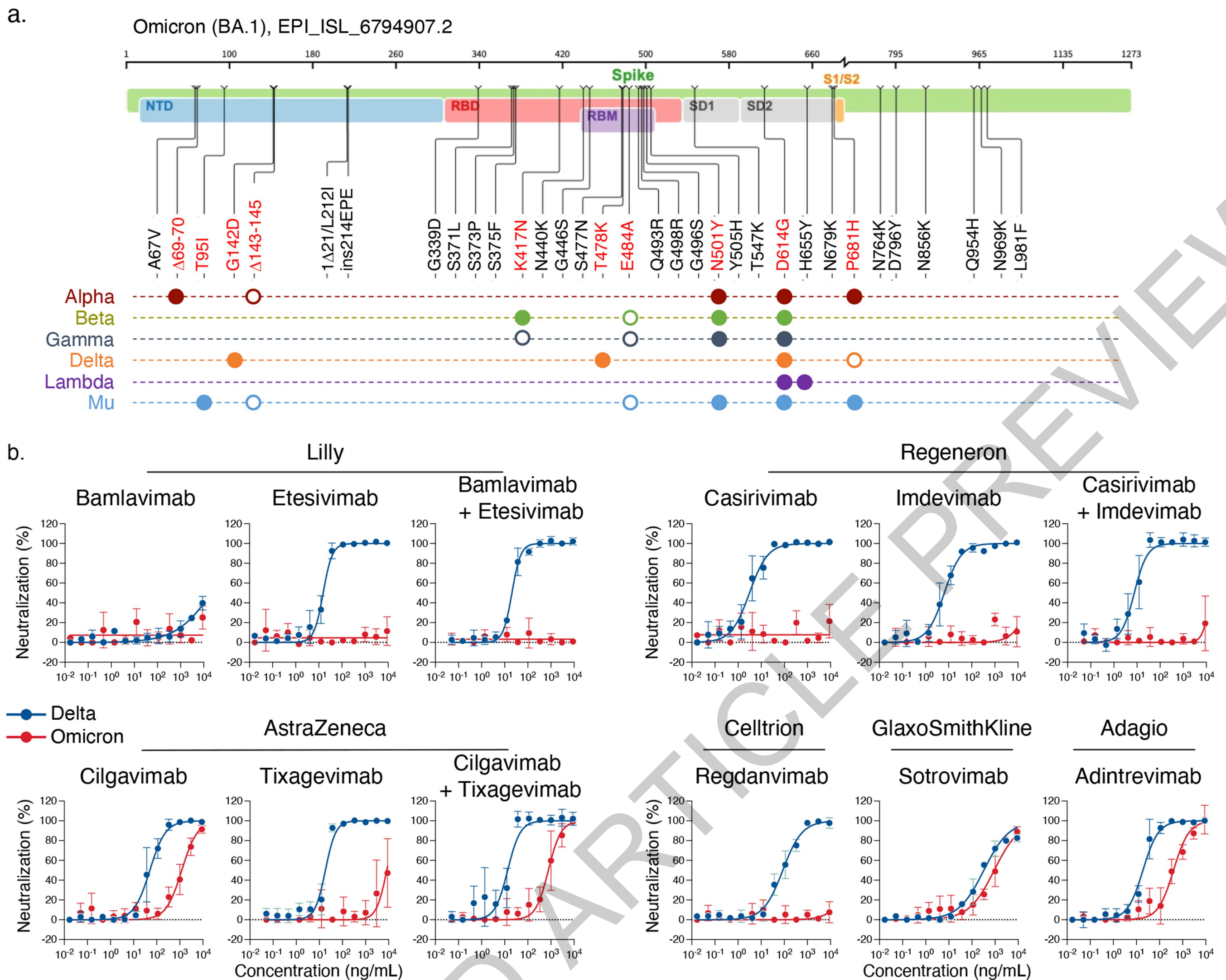


**Fig. 1 | Neutralization of SARS-CoV-2 variants Delta and Omicron by clinical and pre-clinical mAbs. a. Mutational landscape of the Omicron spike**. The amino acid modifications are indicated in comparison to the ancestral Wuhan-Hu-1 sequence (NC_045512). Consensus sequences of the spike protein were built with the Sierra tool[38]. The Omicron sequence corresponds to the viral strain isolated in Belgium and used in the study (GISAID accession ID: (EPI_ISL_6794907). Mutations are compared to some preexisting variants of concern and variants of interest. Filled circles: change identical to Omicron. Open circles: different substitution at the same position. **b. Neutralization curves of mAbs**. Dose response analysis of the neutralization by clinical or pre-clinical mAbs (Bamlanivimab, Etesivimab, Casirivimab, Imdevimab, Adintrevimab, Cligavimab, Tixagevimab, Regdanvimab, Sotrovimab) and the indicated combinations (Bamlanivimab + Etesivimab, Casirivimab + Imdevimab [corresponding to mAbs present in Ronapreve™], Cligavimab+Tixagevimab [corresponding to mAbs present in Evusheld™]) on Delta (blue dots) and Omicron (red dots) variants. Data are mean±SD of 3 independent experiments. For each antibody, the IC50 are presented in Extended Data Table 1.

ACCELERATED ARTICLE PREVIEW

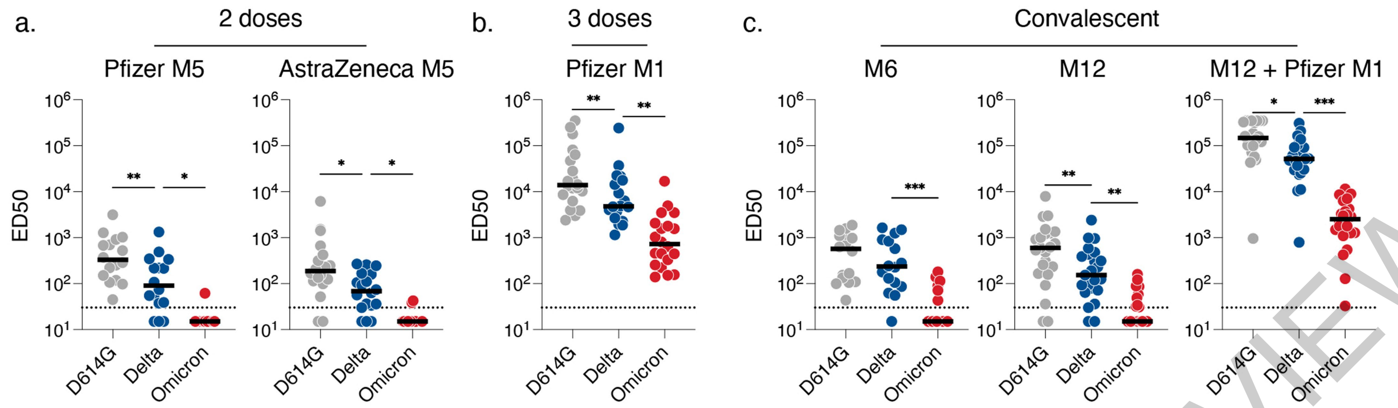


**Fig. 2 | Sensitivity of SARS-CoV-2 variants D614G, Delta and Omicron to sera from vaccinated, convalescent or infected then vaccinated individuals.** Neutralization titers of the sera against the three indicated viral variants are expressed as ED50 (Effective Dose 50%). **a.** Neutralizing activity of sera from AstraZeneca (n=18) (left panel) and Pfizer (n=16) (right panel) vaccinated recipients sampled at 5 months post-second dose. **b.** Neutralizing activity of sera from Pfizer vaccinated recipients sampled one month (M1) after the 3rd injection (n=20). The dotted line indicates the limit of detection (ED50=30). **c.** Neutralizing activity of sera from convalescent individuals (n=16), sampled at 6 months post onset of symptoms (right panel). Neutralizing activity of sera from convalescent individuals (n=23), sampled at 12 months post onset of symptoms (middle panel). Neutralizing activity of sera from infected then vaccinated individuals (n=22), sampled one month after the 1st injection (right panel). In each panel, data are mean from 2 to 3 independent experiments. Two-sided Friedman test with Dunn's multiple comparison was performed to compare D614G and Omicron to the Delta variant. *p<0.05, **p<0.01, ***p<0.001.

ACCELERATED ARTICLE PREVIEW

# Methods

No statistical methods were used to predetermine sample size. The experiments were not randomized and the investigators were not blinded to allocation during experiments and outcome assessment. Our research complies with all relevant ethical regulation.

Orléans Cohort of convalescent and vaccinated individuals. Since August 27, 2020, a prospective, monocentric, longitudinal, interventional cohort clinical study enrolling 170 SARS-CoV-2-infected individuals with different disease severities, and 59 non-infected healthy controls is on-going, aiming to describe the persistence of specific and neutralizing antibodies over a 24-months period. This study was approved by the ILE DE FRANCE IV ethical committee. At enrolment, written informed consent was collected and participants completed a questionnaire which covered sociodemographic characteristics, virological findings (SARS-CoV-2 RT-PCR results, including date of testing), clinical data (date of symptom onset, type of symptoms, hospitalization), and data related to anti-SARS-CoV-2 vaccination if ever (brand product, date of first and second doses). Serological status of participants was assessed every 3 months. Those who underwent anti-SARS-CoV-2 vaccination had regular blood sampling after first dose of vaccine (ClinicalTrials.gov Identifier: NCT04750720). The primary outcome was the presence of antibodies to SARS-CoV-2 spike protein as measured with the S-Flow assay. The secondary outcome was the presence of neutralizing antibodies as measured with the S-Fuse assay. For the present study, we selected 61 convalescent and 54 vaccinated participants. Some individuals were sampled multiple times. We analyzed a total of 115 sera. Study participants did not receive any compensation. The characteristics of each individual from the two cohorts are presented in the supplementary Table 2. The cohorts were constituted before the occurrence of the Omicron variant.

## Phylogenetic analysis

To contextualize the isolated Omicron genome, all SARS-CoV-2 sequences available on the GISAID EpiCov™ database as of December 06, 2021 were retrieved. A subset of complete and high coverage sequences, as indicated in GISAID, assigned to lineages B.1.529 or BA.1 and BA.2 were randomly subsampled. This subset was included in a global SARS-CoV-2 phylogeny reconstructed with augur and visualized with auspice as implemented in the Nextstrain pipeline (https://github.com/nextstrain/ncov, version from May 06, 2021)[39]. Within Nextstrain, a random subsampling approach capping a maximum number of sequences per global region was used. The acknowledgment of contributing and originating laboratories for all sequences used in the analysis is provided in Supplementary Table 1.

## 3D representation of mutations on B1.617.2 and other variants to the spike surface

Panels in Extended Data Fig. 3 were prepared with The PyMOL Molecular Graphics System, Version 2.1 Schrödinger, LLC. The atomic model used (PDB:6XR8) has been previously described[41].

## S-Fuse neutralization assay

U2OS-ACE2 GFP1-10 or GFP 11 cells, also termed S-Fuse cells, become GFP+ when they are productively infected by SARS-CoV-2[12,13]. Cells were tested negative for mycoplasma. Cells were mixed (ratio 1:1) and plated at 8x$10^3$ per well in a μClear 96-well plate (Greiner Bio-One). The indicated SARS-CoV-2 strains were incubated with serially diluted mAb or sera for 15 minutes at room temperature and added to S-Fuse cells. The sera were heat-inactivated 30 min at 56 °C before use. 18 hours later, cells were fixed with 2% PFA, washed and stained with Hoechst (dilution 1:1,000, Invitrogen). Images were acquired with an Opera Phenix high content confocal microscope (PerkinElmer). The GFP area and the number of nuclei were quantified using the Harmony software (PerkinElmer). The percentage of neutralization was calculated using the number of syncytia as value with the following formula: 100 x (1 – (value with serum – value in "non-infected")/(value in "no serum" – value in "non-infected")). Neutralizing activity of each serum was expressed as the half maximal effective dilution (ED50). ED50 values (in μg/ml for mAbs and in dilution values for sera) were calculated with a reconstructed curve using the percentage of the neutralization at the different concentrations.

## Characteristics of the patient infected with Omicron

The 32-year-old woman was unvaccinated and developed moderate symptoms on November 22, 2021, 11 days after returning to Belgium from Egypt via Turkey (stop-over to switch flights, without having left the airport). She did not display any risk factor for severe COVID-19 and rapidly recovered. She transmitted the virus to her husband but not to their children. She provided informed written consent to use the swab for future studies. The nasopharyngeal swab tested positive for SARS-CoV-2 on this date. The leftover material of the sample was used in this study after performing routine diagnostics, within the context of the mandate that was provided to UZ/KU Leuven as National Reference Center (NRC) of respiratory pathogens, as described in detail in the Belgian Royal Decree of 09/02/2011.

## Virus strains

The reference D614G strain (hCoV-19/France/GE1973/2020) was supplied by the National Reference Centre for Respiratory Viruses hosted by Institut Pasteur (Paris, France) and headed by Pr. S. van der Werf. This viral strain was supplied through the European Virus Archive goes Global (Evag) platform, a project that has received funding from the European Union's Horizon 2020 research and innovation program under grant agreement n° 653316. The variant strains were isolated from nasal swabs using Vero E6 cells and amplified by one or two passages. Delta was isolated from a nasopharyngeal swab of a hospitalized patient returning from India[14]. The swab was provided and sequenced by the laboratory of Virology of Hopital Européen Georges Pompidou (Assistance Publique – Hopitaux de Paris). The Omicron-positive sample was cultured on Vero E6 cells as previously described[42] Viral growth was confirmed by RT-qPCR 3 days post-infection (p.i.). At day 6 p.i., a cytopathic effect (CPE) was detected and a full-length sequencing of the virus was performed. The Omicron strain was supplied and sequenced by the NRC UZ/KU Leuven (Leuven, Belgium). Both patients provided informed consent for the use of the biological materials. Titration of viral stocks was performed on Vero E6, with a limiting dilution technique allowing a calculation of TCID50, or on S-Fuse cells. Viruses were sequenced directly on nasal swabs, and after one or two passages on Vero cells. Sequences were deposited on GISAID immediately after their generation, with the following IDs: D614G: EPI_ISL_414631; Delta ID: EPI_ISL_2029113; Omicron ID: EPI_ISL_6794907.

## Flow Cytometry

Vero cells were infected with the indicated viral strains at a multiplicity of infection (MOI) of 0.01. Two days after, cells were detached using PBS-0.1%EDTA and transferred into U-bottom 96-well plates (50,000 cells/well). Cells were then incubated for 30 min at 4 °C with the indicated mAbs (1 or 0.1 μg/mL) in MACS buffer (PBS, 5g/L BSA, 2mM EDTA). Cells were washed with PBS and stained using anti-IgG AF647 (1:600 dilution in MACS buffer) (ThermoFisher). Stainings were also performed on control non-infected (NI) cells. Cells were then fixed in 4% PFA for 30 min at RT. Data were acquired on an Attune Nxt instrument using Attune Nxt Software v3.2.1 (Life Technologies) and analysed with FlowJo 10.7.1 (Becton Dickinson).

## Antibodies

Four clinically available antibodies (Bamlavimab, Casirivimab, Etesevimab and Imedvimab) were kindly provided by CHR Orleans. The other human SARS-CoV-2 anti-RBD neutralizing antibodies (ADG2 or

ACCELERATED ARTICLE PREVIEW

Adintrevimab, AZD1061 (COV2-2130) or Cilgavimab, AZD8895 (COV2-2196) or Tixagevimab, CT-P59 or Regdanvimab, LY-CoV016 (CB6) or Etesevimab, LY-CoV555 or Bamlanivimab, REGN10933 or Casirivimab, REGN10987 or Imdevimab, and VIR-7831 (S309) or Sotrovimab[19–25] were produced as followed. DNA fragments coding for their IgH and IgL variable domains were synthetized (Life Technologies, Thermo Fisher Scientific). Purified digested DNA fragments were cloned into human Igγ1- and Ig κ- / Igλ-expressing vectors[43] and recombinant IgG1 antibodies were produced by transient co-transfection of Freestyle™ 293-F suspension cells (Thermo Fisher Scientific) using PEI-precipitation method as previously described[44]. IgG1 antibodies were purified by batch/gravity-flow affinity chromatography using protein G sepharose 4 fast flow beads (Cytivia) according to the manufacturer's instructions, dialyzed against PBS using Slide-A-Lyzer® dialysis cassettes (Thermo Fisher Scientific), quantified using NanoDrop 2000 instrument (Thermo Fisher Scientific) and checked for purity and quality on a silver-stained SDS-PAGE gel (3-8% Tris-Acetate Novex, Thermo Fisher Scientific). The pan-coronavirus anti-S2 non-neutralizing antibody Ab-10 was previously described[13,14].

### Statistical analysis

Flow cytometry data were analyzed with FlowJo v10 software (TriStar). Calculations were performed using Excel 365 (Microsoft). Figures were drawn on Prism 9 (GraphPad Software). Statistical analysis was conducted using GraphPad Prism 9. Statistical significance between different groups was calculated using the tests indicated in each figure legend.

### Reporting summary

Further information on research design is available in the Nature Research Reporting Summary linked to this paper.

## Data availability

All data supporting the findings of this study are available within the article or from the corresponding authors upon request. Source data are provided with this paper. Viral sequences are available upon request and were deposited at GISAID (https://www.gisaid.org/) under the following numbers: D614G: EPI_ISL_414631; Delta ID: EPI_ISL_2029113; Omicron ID: EPI_ISL_6794907. Source data are provided with this paper.


39. Hadfield, J. et al. Nextstrain: real-time tracking of pathogen evolution. *Bioinformatics* **34**, 4121-4123, https://doi.org/10.1093/bioinformatics/bty407 (2018).
40. Walls, A. C. et al. Structure, Function, and Antigenicity of the SARS-CoV-2 Spike Glycoprotein. *Cell* **181**, 281-292 e286, https://doi.org/10.1016/j.cell.2020.02.058 (2020).
41. Cai, Y. et al. Distinct conformational states of SARS-CoV-2 spike protein. *Science* **369**, 1586-1592, https://doi.org/10.1126/science.abd4251 (2020).
42. Van Cleemput, J. et al. Organ-specific genome diversity of replication-competent SARS-CoV-2. *Nature Communications* **12**, 6612, https://doi.org/10.1038/s41467-021-26884-7 (2021).
43. Tiller, T. et al. Efficient generation of monoclonal antibodies from single human B cells by single cell RT-PCR and expression vector cloning. *Journal of Immunological Methods* **329**, 112-124, https://doi.org/10.1016/j.jim.2007.09.017 (2008).
44. Lorin, V. & Mouquet, H. Efficient generation of human IgA monoclonal antibodies. *Journal of Immunological Methods* **422**, 102-110, https://doi.org/10.1016/j.jim.2015.04.010 (2015).



**Acknowledgements** We thank the European Health Emergency Preparedness and Response Authority, (HERA) for its support. We thank Stewart Cole for his help in initiating the collaboration between Institut Pasteur and KU Leuven through the HERA network. We thank Artem Baidaliuk and Fabiana Gambaro for their help with the sequencing data analysis. We thank patients who participated to this study, members of the Virus and Immunity Unit and other teams for discussions and help, Nathalie Aulner and the UtechS Photonic BioImaging (UPBI) core facility (Institut Pasteur), a member of the France BioImaging network, for image acquisition and analysis. The Opera system was co-funded by Institut Pasteur and the Région ile de France (DIM1Health). We thank the KU Leuven University authorities and Jef Arnout, Bruno Lambrecht, Chris Van Geet and Luc Sels for their support. We thank Laurent Belec, Nicolas Robillard and Madelina Saliba for their help with sequencing. We thank Fabienne Peira, Vanessa Legros and Laura Courtellemont for their help with the cohorts. Work in OS lab is funded by Institut Pasteur, Urgence COVID-19 Fundraising Campaign of Institut Pasteur, Fondation pour la Recherche Médicale (FRM), ANRS, the Vaccine Research Institute (ANR-10-LABX-77), Labex IBEID (ANR-10-LABX-62-IBEID), ANR/FRM Flash Covid PROTEO-SARS-CoV-2 and IDISCOVR. Work in UPBI is funded by grant ANR-10-INSB-04-01 and Région Ile-de-France program DIM1-Health. DP is supported by the Vaccine Research Institute. HM lab is funded by the Institut Pasteur, the Milieu Intérieur Program (ANR-10-LABX-69-01), the INSERM, REACTing, EU (RECOVER) and Fondation de France (#00106077) grants. ESL lab is funded by Institut Pasteur, the INCEPTION program (Investissements d'Avenir grant ANR-16-CONV-0005) and and the French Government's Investissement d'Avenir programme, Laboratoire d'Excellence "Integrative Biology of Emerging Infectious Diseases" (grant n°ANR-10-LABX-62-IBEID). GB acknowledges support from the Internal Funds KU Leuven under grant agreement C14/18/094, and the Research Foundation — Flanders (Fonds voor Wetenschappelijk Onderzoek — Vlaanderen, G0E1420N, G098321N). PM acknowledges support from a COVID19 research grant of 'Fonds Wetenschappelijk Onderzoek'/Research Foundation Flanders (grant G0H4420N). SD is supported by the Fonds National de la Recherche Scientifique (FNRS, Belgium) and also acknowledges support from the Research Foundation - Flanders (Fonds voor Wetenschappelijk Onderzoek-Vlaanderen, G098321N) and from the European Union Horizon 2020 project MOOD (grant agreement no.874850).The funders of this study had no role in study design, data collection, analysis and interpretation, or writing of the article.


**Author contributions** Experimental strategy design, experiments: DP, NS, FGB, CP, JB, WHB, FP, IS, FR, ESL, TB, HM, OS Vital materials: PM, CP, FL, HP, DV, JP, JR, GB, SD, JR, SG, CG, BV, TWB, JMC, LC, AS, LH, TP, HM, EA Phylogenetic analysis: GB, ESL, FL, SD Manuscript writing: DP, FR, ESL, TB, HM, EA, OS Manuscript editing: DP, NS, PM, GB, LC, FR, ESL, TB, HM, EA, OS.

**Competing interests** C.P., H.M., O.S, T.B., F.R. have a pending patent application for an anti-RBD mAb not used in this study (PCT/FR2021/070522).

**Additional information**

**Supplementary information** The online version contains supplementary material available at https://doi.org/10.1038/s41586-021-04389-z.

**Correspondence and requests for materials** should be addressed to Timothée Bruel, Hugo Mouquet, Emmanuel André or Olivier Schwartz.


**Peer review information** *Nature* thanks the anonymous reviewers for their contribution to the peer review of this work.



**Reprints and permissions information** is available at http://www.nature.com/reprints.

ACCELERATED ARTICLE PREVIEW

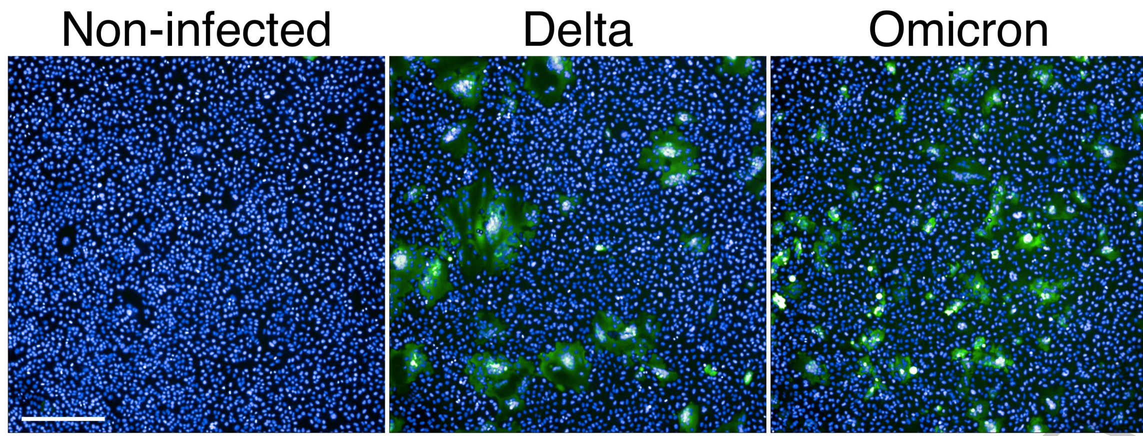


**Extended Data Fig. 1 | SARS-CoV-2 variants induce syncytia in S-Fuse cells.** S-Fuse cells were exposed to the indicated SARS-CoV-2 strains, at a multiplicity of infection (MOI) of $10^{-3}$. The cells become GFP+ when they fuse together. After 20 h, infected cells were stained with Hoechst to visualize nuclei. Syncytia (green) and nuclei (blue) are shown. Representative images from three independent experiments are shown. Scale bar, 500 µm.

ACCELERATED ARTICLE PREVIEW

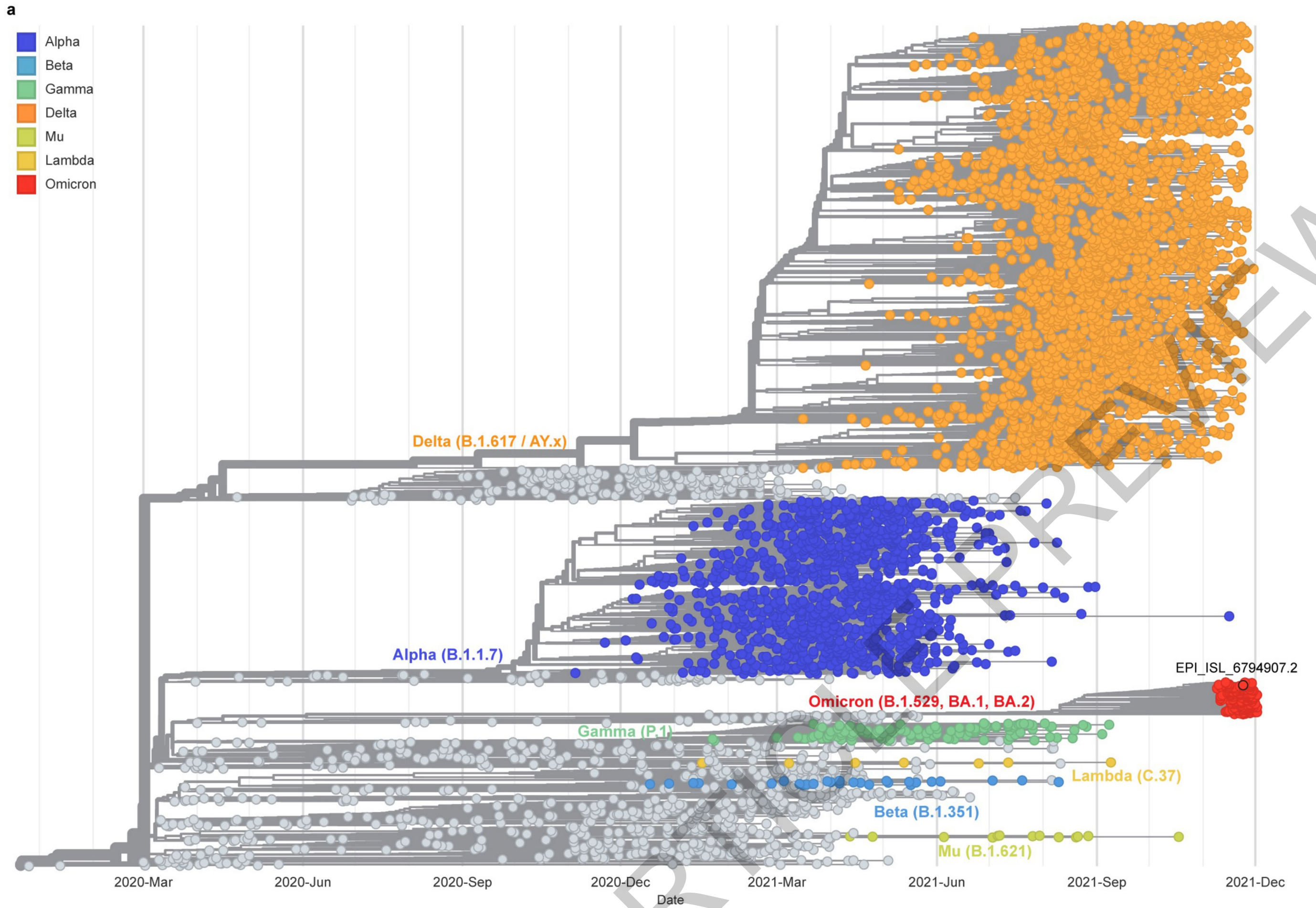


**Extended Data Fig. 2 | Global phylogeny of SARS-CoV-2 highlighting the Omicron lineage.** Time calibrated global SARS-CoV-2 phylogeny available from the Nextstrain platform (https://nextstrain.org/ncov/gisaid/global)[39]. The position of the isolated Omicron variant is highlighted, and the variants of concern (VOCs) (Alpha, Beta, Gamma, Delta and Omicron) and variants of interest (VOIs) (Lambda, Mu) are colored as indicated.

ACCELERATED ARTICLE PREVIEW

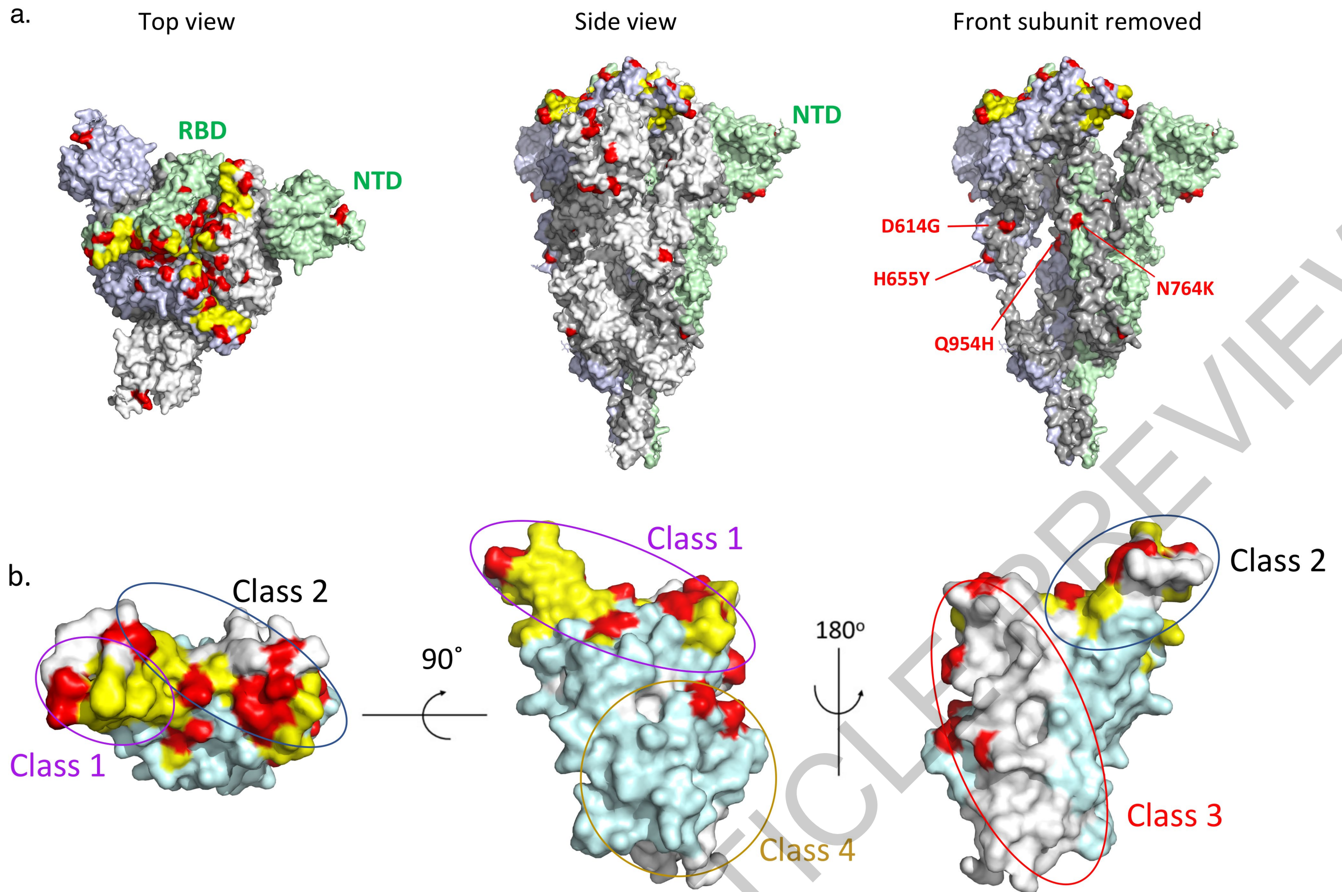


**Extended Data Fig. 3 | Mapping of the mutations present in Omicron to the spike's surface. a**. The spike shown in top (left panel) and in side view (middle and right panels). The spike trimer is shown in surface representation with the three protomers colored in light grey, light blue and light green. N-terminal and the receptor-binding (NTD and RBD) domains are labeled for the protomer in green only. The represented spike (PDB: 6XR8) is in the closed conformation, i.e., with all three RBDs in the "Down" conformation[40]. The RBD surface of interaction with hACE2 (which is partially occluded in a closed spike) is colored in yellow. The amino acid differences in the spike of the Omicron variant with respect to the initial Wuhan sequence are marked in red. In the right panel, the front subunit was removed to show changes in S2 and in the C-terminal segment of S1 (labeled) that map to the trimer interface, which could impact the stability of the spike trimer. **b**. The RBD view down the hACE2 binding surface (left panel) and in two other orthogonal orientations (middle and right panel), as indicated. The hACE2 binding surface is colored in yellow and the residues altered in Omicron are in red. The RBD surfaces that are buried and exposed in a closed spike are colored in light cyan and white, respectively. The ovals outline the location of the epitopes of neutralizing antibodies of the various classes that have been described[17].

ACCELERATED ARTICLE PREVIEW

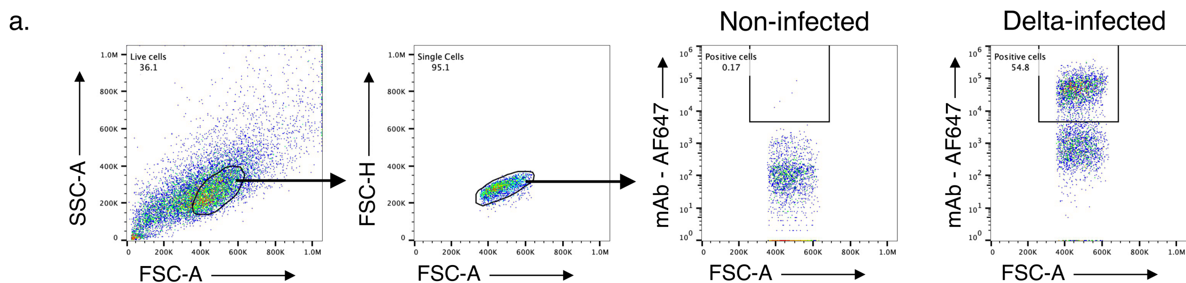


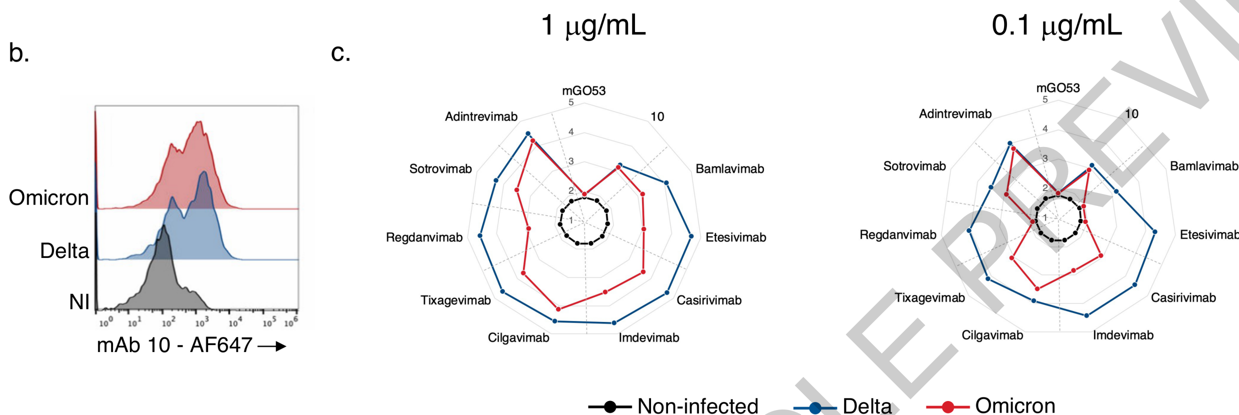


d.

| | | Neutralization (IC50 ng/ml) | | Binding (Fold-decrease Omicron/Delta) | | | |
|---|---|---|---|---|---|---|---|
| | | | | 1 µg/mL | | 0.1 µg/mL | |
| | | Delta | Omicron | Delta | Omicron | Delta | Omicron |
| Lilly | Bamlavimab | >9000 | >9000 | 1 | 8 | 1 | 17 |
| | Etesivimab | 15.4 | >9000 | 1 | 42 | 1 | 242 |
| | Bamla/Ete | 20.5 | >9000 | 1 | n.d | 1 | n.d |
| Regeneron | Casirivimab | 3.1 | >9000 | 1 | 12 | 1 | 32 |
| | Imdevimab | 6.5 | >9000 | 1 | 12 | 1 | 39 |
| | Casirivimab/Imdevimab | 7.6 | >9000 | 1 | n.d | 1 | n.d |
| AstraZeneca | Cilgavimab | 50.3 | 1213 | 1 | 3 | 1 | 3 |
| | Tixagevimab | 18.3 | 8305 | 1 | 9 | 1 | 11 |
| | Cilgavimab/Tixagevimab | 13.4 | 773 | 1 | n.d | 1 | n.d |
| Celltrion | Regdanvimab | 86.6 | >9000 | 1 | 2 | 1 | 2 |
| GlaxoSmithKline | Sotrovimab | 325 | 917 | 1 | 6 | 1 | 4 |
| Adagio | Adintrevimab | 19.6 | 403 | 1 | 47 | 1 | 145 |

**Extended Data Fig. 4 | Binding of anti-SARS-CoV-2 monoclonal antibodies to Vero cells infected with Delta and Omicron variants.** Vero cells were infected with the indicated variants at an MOI of 0.01. After 48 h, cells were stained with 1 or 0.1 µg/mL of the indicated anti-SARS-CoV-2 monoclonal antibodies (Bamlanivimab, Etesivimab, Casirivimab, Imdevimab, Adintrevimab, Cligavimab, Tixagevimab, Regdanvimab, Sotrovimab) and analysed by flow-cytometry. **a**. Gating strategy and example of gates on negative (non-infected) or positive (Delta-infected) samples. **b**. The anti-S2 pan-coronavirus mAb 10 was used to measure the percentage of infected cells. Histograms show binding of mAb 10 to Vero cells infected with the indicated variants. **c**. Radar charts represent for each antibody the logarithm of the median fluorescent intensity (MFI) of the staining. Data are representative of two or three independent experiments. **d**. Inhibitory Concentrations 50% (IC50) of mAbs against Delta and Omicron variants. The IC50 of the indicated mAbs and some of their combinations were calculated from the neutralization curves displayed in Fig. 1b. Results are in ng/mL. Color code: Grey: inactive mAbs. Green: mAbs displaying a neutralizing activity. The binding activity was measured by flow cytometry on Vero cells infected with the indicated variants. Results are presented as the fold-decrease of binding to Omicron-infected cells relative to Delta-infected cells.

ACCELERATED ARTICLE PREVIEW

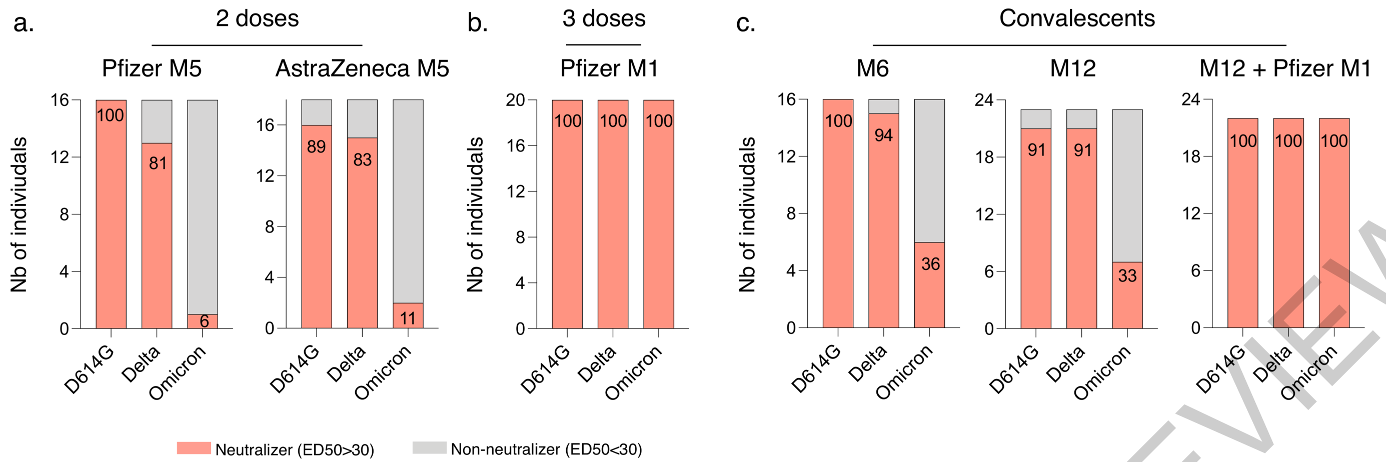


**Extended Data Fig. 5 | Fraction of neutralizers in the cohorts of vaccinated or convalescent individuals.** Individuals with an ED50 of neutralization above 30 were categorized as neutralizers and are indicated in pink. Non-neutralizers are in grey. The numbers indicate the percentage of neutralizers. **a.** Fraction of neutralizers in sera from Pfizer (n=16) (left panel) and AstraZeneca (n=18) (right panel) vaccinated recipients sampled 5 months after the second dose (results related to Fig. 2a). **b.** Fraction of neutralizers in sera from Pfizer vaccinated recipients sampled one month after the 3rd injection (n=20; (results related to Fig. 2b). **c.** Fraction of neutralizers in sera from convalescent individuals, sampled at 6 months post onset of symptoms (M6) (n=16) (right panel), at 12 months (M12) (n=23) (middle panel) and one month after the 1st injection (n=22) (right panel; results related to Fig. 2c). In each panel, data are mean from 2 to 3 independent experiments.

ACCELERATED ARTICLE PREVIEW

**Extended Data Table 1 | Characteristics of the two cohorts of vaccinated and convalescent individuals**

a. Vaccinees

| | | AstraZeneca M5 (2 doses) n=18 | Pfizer M5 (2 doses) n=16 | Pfizer M1 (3 doses) n=20 |
|---|---|---|---|---|
| Sex | | | | |
| | Female | 12 | 6 | 9 |
| | Male | 6 | 10 | 11 |
| Age (median; range) | | 60 (55;78) | 53 (33;74) | 53 (33;74) |
| Immune deficiency | | 0 | 0 | 0 |
| Previous COVID-19 | | 0 | 0 | 0 |
| Anti-N | | 0 | 0 | 0 |
| 1st shot | | Feb 5 – April 7, 2021 | Jan 6- Feb 4,2021 | Jan 6- April12,2021 |
| 2nd shot | | May3-19, 2021 | Jan 28 - March 3, 2021 | Jan 28 – May 8, 2021 |
| 3rd shot | | - | - | July 1 –Nov 25, 2021 |
| Sampling days post-2nd dose; M5 (median; range) | | 150 (110-178) | 161 (138-176) | - |
| Sampling days post-3rd dose; M1 (median; range) | | - | - | 33 (8-61) |

b. Convalescents

| | | 6M POS n=16 | 12M POS n=23 | 12M POS then vaccinated n=22 |
|---|---|---|---|---|
| Sex | | | | |
| | Female | 10 | 11 | 11 |
| | Male | 6 | 12 | 11 |
| Age (Median; range) | | 56 (32;77) | 52 (23;82) | 52 (23 ;82) |
| Severity | | | | |
| | Severe | 8 | 13 | 9 |
| | Mild-Moderate | 7 | 8 | 4 |
| | Asymptomatic | 1 | 2 | 1 |
| PCR | | 15 | 21 | 20 |
| Anti-S (S-Flow) | | 16 | 23 | 22 |
| Sampling days POS (median; range) | | 184 (129;195) | 368 (344-454) | - |
| Days between the vaccination and onset of symptoms (median; range) | | - | - | 394 (353-444) |
| Sampling days post-vaccination (median; range) | | - | - | 32 (21-48) |

ACCELERATED ARTICLE PREVIEW

nature research

Corresponding author(s): Olivier Schwartz, Timothée Bruel, Emmanuel André

Last updated by author(s): Dec 13, 2021

# Reporting Summary

Nature Research wishes to improve the reproducibility of the work that we publish. This form provides structure for consistency and transparency in reporting. For further information on Nature Research policies, see our Editorial Policies and the Editorial Policy Checklist.

## Statistics

For all statistical analyses, confirm that the following items are present in the figure legend, table legend, main text, or Methods section.

| n/a | Confirmed | |
|---|---|---|
| ☐ | ☒ | The exact sample size (*n*) for each experimental group/condition, given as a discrete number and unit of measurement |
| ☐ | ☒ | A statement on whether measurements were taken from distinct samples or whether the same sample was measured repeatedly |
| ☐ | ☒ | The statistical test(s) used AND whether they are one- or two-sided<br>*Only common tests should be described solely by name; describe more complex techniques in the Methods section.* |
| ☐ | ☒ | A description of all covariates tested |
| ☐ | ☒ | A description of any assumptions or corrections, such as tests of normality and adjustment for multiple comparisons |
| ☐ | ☒ | A full description of the statistical parameters including central tendency (e.g. means) or other basic estimates (e.g. regression coefficient) AND variation (e.g. standard deviation) or associated estimates of uncertainty (e.g. confidence intervals) |
| ☐ | ☒ | For null hypothesis testing, the test statistic (e.g. *F*, *t*, *r*) with confidence intervals, effect sizes, degrees of freedom and *P* value noted<br>*Give P values as exact values whenever suitable.* |
| ☒ | ☐ | For Bayesian analysis, information on the choice of priors and Markov chain Monte Carlo settings |
| ☒ | ☐ | For hierarchical and complex designs, identification of the appropriate level for tests and full reporting of outcomes |
| ☒ | ☐ | Estimates of effect sizes (e.g. Cohen's *d*, Pearson's *r*), indicating how they were calculated |

*Our web collection on statistics for biologists contains articles on many of the points above.*

## Software and code

Policy information about availability of computer code

| | |
|---|---|
| Data collection | Harmony Software v4.9 (Perkin-Elmer), Attune Nxt Software v3.2.1 (ThermoFischer), Flowjo Software v10.7.1 |
| Data analysis | Excel 365 v16.46 (Microsoft), Prism v9.0.2 (GraphPad Software) |

For manuscripts utilizing custom algorithms or software that are central to the research but not yet described in published literature, software must be made available to editors and reviewers. We strongly encourage code deposition in a community repository (e.g. GitHub). See the Nature Research guidelines for submitting code & software for further information.

## Data

Policy information about availability of data

All manuscripts must include a data availability statement. This statement should provide the following information, where applicable:

- Accession codes, unique identifiers, or web links for publicly available datasets
- A list of figures that have associated raw data
- A description of any restrictions on data availability

All data associated with this study are available from O.S

# Field-specific reporting

Please select the one below that is the best fit for your research. If you are not sure, read the appropriate sections before making your selection.

☒ Life sciences ☐ Behavioural & social sciences ☐ Ecological, evolutionary & environmental sciences

For a reference copy of the document with all sections, see nature.com/documents/nr-reporting-summary-flat.pdf

# Life sciences study design

All studies must disclose on these points even when the disclosure is negative.

| | |
|---|---|
| Sample size | 131 sera from convalescent, vaccinated and vaccinated convalescent individuals were analyzed in the study. Given the explanatory nature of the study aiming at describing a phenomenon whose frequency has not yet been established it was not possible to use statistical methods were used to predetermine sample size. Thus, we included between 10 and 50 patients per group. |
| Data exclusions | None. |
| Replication | All experiments were performed and verified in multiple replicates as indicated in their methods/figure legends. |
| Randomization | The experiments were not randomized as we tested all available samples. |
| Blinding | The investigators were not blinded to allocation during experiments and outcome assessment. However, the clinical sampling and biological measurement were performed by different teams. Only the final assembly of the data revealed the global view of the results. |

# Reporting for specific materials, systems and methods

We require information from authors about some types of materials, experimental systems and methods used in many studies. Here, indicate whether each material, system or method listed is relevant to your study. If you are not sure if a list item applies to your research, read the appropriate section before selecting a response.

## Materials & experimental systems

| n/a | Involved in the study | |
|---|---|---|
| ☐ | ☒ | Antibodies |
| ☐ | ☒ | Eukaryotic cell lines |
| ☒ | ☐ | Palaeontology and archaeology |
| ☒ | ☐ | Animals and other organisms |
| ☐ | ☒ | Human research participants |
| ☐ | ☒ | Clinical data |
| ☒ | ☐ | Dual use research of concern |

## Methods

| n/a | Involved in the study | |
|---|---|---|
| ☒ | ☐ | ChIP-seq |
| ☐ | ☒ | Flow cytometry |
| ☒ | ☐ | MRI-based neuroimaging |

## Antibodies

| | |
|---|---|
| Antibodies used | Adintrevimab, Cilgavimab, Regdavimab, Sotrovimab and Tixagevimab are human anti-S monoclonal antibodies produced by Hugo Mouquet (Institut Pasteur). Bamlanivimab, Etesivimab, Casirivimab and Imdevimab were kind gifts of Thierry Prazuck and Laurent Hocqueloux. The Goat anti-Human IgG (H+L) Cross-Adsorbed Secondary Antibody, Alexa Fluor 647 (A21445) was obtained from thermoFisher Scientific. |
| Validation | Adintrevimab, Cilgavimab, Regdavimab, Sotrovimab and Tixagevimab were validated using ELISA binding assays (against the trimeric S, RBD, and S2 proteins) by the team of H.Mouquet. Bamlanivimab, Etesivimab, Casirivimab and Imdevimab were validated by measuring their neutralizing activity against SARS-CoV-2. Validation of the goat anti-human IgG is available from the ThermoFisher website. |

## Eukaryotic cell lines

Policy information about cell lines

| | |
|---|---|
| Cell line source(s) | Vero E6 (ATCC® CRL-1586™), 293T cells (ATCC CRL- 3216), Freestyle 293-F (ThermoFisher) and U2OS cells (ATCC® HTB-96™), all obtained from the ATCC. |
| Authentication | Cell lines were not authenticated. |
| Mycoplasma contamination | All cells are negative for mycoplasma contamination. Tests are performed every Monday. |

| | |
|---|---|
| Commonly misidentified lines (See ICLAC register) | None |

## Human research participants

Policy information about studies involving human research participants

| | |
|---|---|
| Population characteristics | Orleans' Cohort of convalescent and/or vaccinated individuals: since April 2020, a prospective, monocentric, longitudinal, cohort clinical study enrolling 170 SARS-CoV-2-infected individuals and 30 non-infected healthy controls is on-going, aiming to describe the persistence of specific and neutralizing antibodies over a 24-months period.<br>Given the exploratory design of the study, the characteristics of participants were not pre-established when entering the cohorts. Relevant co-variates are provided in the corresponding supplementary tables. |
| Recruitment | Orléans cohort : Individuals admitted to the hospital for COVID-19 vaccination, COVID-19 or with known COVID-19 consulting for a chronic disease were invited to participate.<br>Individuals were included without any selection other than those imposed by the entry criteria (known COVID-19 or vaccination). Under these conditions, no particular bias is envisaged. |
| Ethics oversight | Orléans was approved by national external committee (CPP Ile de France IV, IRB No. 00003835). At enrolment a written informed consent was collected for all participants. |

Note that full information on the approval of the study protocol must also be provided in the manuscript.

## Clinical data

Policy information about clinical studies

All manuscripts should comply with the ICMJE guidelines for publication of clinical research and a completed CONSORT checklist must be included with all submissions.

| | |
|---|---|
| Clinical trial registration | NCT04750720 |
| Study protocol | All protocols can be accessed on clinicaltrial.gov |
| Data collection | The cohort started on April 2020 in Orléans Hospital (Centre hospitalier Réginal Orléans), and is on-going. |
| Outcomes | The primary outcome of the study was the presence of antibody to SARS-CoV-2 antibody binding to the spike protein (S-Flow assay).<br>The secondary outcome of the assay was the presence of neutralizing antibodies (S-Fuse assay) |

## Flow Cytometry

### Plots

Confirm that:

☒ The axis labels state the marker and fluorochrome used (e.g. CD4-FITC).

☒ The axis scales are clearly visible. Include numbers along axes only for bottom left plot of group (a 'group' is an analysis of identical markers).

☒ All plots are contour plots with outliers or pseudocolor plots.

☒ A numerical value for number of cells or percentage (with statistics) is provided.

### Methodology

| | |
|---|---|
| Sample preparation | SARS-CoV-2 infected Vero cells were stained as indicated in the method section. All samples were acquired within 24h. |
| Instrument | Attune NxT Acoustic Focusing Cytometer, blue/red/violet/yellow (catalog number : 15360667) |
| Software | AttuneNxT Software v3.2.1 |
| Cell population abundance | At least 10,000 cells were acquired for each condition. |
| Gating strategy | All gates were set on uninfected Vero cells. |

☒ Tick this box to confirm that a figure exemplifying the gating strategy is provided in the Supplementary Information.